www.elsevier.com/locate/jssc

Acidic 1,3-propanediaminetetraacetato lanthanides with luminescent and catalytic ester Hydrolysis properties

Mao-Long Chen, Yu-Chen Yang, Zhao-Hui Zhou

PII: S0022-4596(14)00342-9
DOI: http://dx.doi.org/10.1016/j.jssc.2014.07.037
Reference: YJSSC18573

To appear in: *Journal of Solid State Chemistry*

Received date: 17 May 2014
Revised date: 17 July 2014
Accepted date: 27 July 2014

Cite this article as: Mao-Long Chen, Yu-Chen Yang, Zhao-Hui Zhou, Acidic 1,3-propanediaminetetraacetato lanthanides with luminescent and catalytic ester Hydrolysis properties, *Journal of Solid State Chemistry*, http://dx.doi.org/10.1016/j.jssc.2014.07.037

Acidic 1,3-propanediaminetetraacetato lanthanides with luminescent and catalytic ester hydrolysis properties

Mao-Long Chen, Yu-Chen Yang, Zhao-Hui Zhou*

College of Chemistry and Chemical Engineering, State Key Laboratory of Physical Chemistry of Solid Surfaces, Xiamen University, Xiamen 361005, China

Abstract

In acidic solution, a serials of water-soluble coordination polymers were isolated as zonal 1D-CPs 1,3-propanediaminetetraacetato lanthanides $[Ln(1,3\text{-}H_3pdta)(H_2O)_5]_n{\cdot}2Cl_n{\cdot}3nH_2O$ [Ln = La, **1**; Ce, **2**; Pr, **3**; Nd, **4**; Sm, **5**] (1,3-H_4pdta = 1,3-propanediaminetetraacetatic acid, $C_{11}H_{18}N_2O_8$) in high yields. When 1 eq. mole potassium hydroxide was added to the solutions of 1D-CPs respectively, two 1D-CPs $[Ln(1,3\text{-}H_2pdta)(H_2O)_3]_n{\cdot}Cl_n{\cdot}2nH_2O$ [Ln = Sm, **6**; Gd, **7**] were isolated at room temperature and seven 2D-CPs $[Ln(1,3\text{-}H_2pdta)(H_2O)_2]_n{\cdot}Cl_n{\cdot}2nH_2O$ [Ln = La, **8**; Ce, **9**; Pr, **10**; Nd, **11**; Sm, **12**; Eu, **13**; Gd, **14**] were isolated at 70 °C. When the crystals of **1**−**4** were hydrothermally heated at 180 °C with 1-2 eq. mole potassium hydroxide, four 3D-CPs $[Ln(1,3\text{-}Hpdta)]_n{\cdot}nH_2O$ [Ln = La, **15**; Ce, **16**; Pr, **17**; Nd, **18**] were obtained. The two 2D-CPs $[Ln(1,3\text{-}Hpdta)(H_2O)]_n{\cdot}4nH_2O$ (Sm, **19**; Eu, **20**) were isolated in similar reaction condition. With the increments of pH value in the solution and reaction temperature, the structure becomes more complicated. **1**−**5** are soluble in water and **1** was traced by solution $^{13}C\{^1H\}$ NMR technique, the water-soluble lanthanides **1** and **5** show catalytic activity to ester hydrolysis reaction respectively, which indicate their important roles in the hydrolytic reaction. The europium complexes **13** and **20** show visible fluorescence at an excitation of 394 nm. The structure diversity is mainly caused by the variation of coordinated ligand in different pH values and lanthanide contraction effect.

Acidic conditions are favorable for the isolations of lanthanide complexes in different structures and this may helpful to separate different lanthanides. The thermal stability investigations reveal that acidic condition is favorable to obtain the oxides at a lower temperature.

Keywords: Lanthanide; 1,3-propanediaminetetraacetic acid; ester hydrolysis, luminescent

---

* Corresponding author. Tel.: +86 592 2184531; fax: +86 592 2183047 (Z.-H. Zhou).

E-mail address: zhzhou@xmu.edu.cn (Z.-H. Zhou).

1. Introduction

The chemistry of the coordination polymers has in recent years advanced extensively [1-7], where the lanthanides often show applications in many fields such as gas adsorption and separation [8, 9], chemical sensors [10], catalysts [11, 12], magnetic and luminescent materials [1, 6, 13], and so on. However, less concerns are focused on the design and synthesis of water-soluble lanthanide-based coordination polymers which may have special solution state and easy for separations and conversions [14-17].

In general, 1,3-propanediaminetetraacetic acid, which is an edta-like ligand (edta = $[CH_2N(CH_2CO_2H)_2]_2$), is a tetrabasic acid with eight potential O-donor and two N-donor atoms for the formations of mononuclear water-soluble complexes [18]. Usually it coordinates with transition center ions through its four oxygen atoms and two nitrogen atoms, like $M'^{II}(H_2O)_6][M^{II}$(1,3-pdta)]·$2H_2O$ (M = Ca [19], Co [20, 21], Ni [22, 23], Cu [22, 24, 25] and Zn[26]), $[M'^{II}(H_2O)_6][M^{II}$(1,3-pdta)$(H_2O)]\cdot 2H_2O$ (M = Mn [27] and Cd [26, 27]), M'$[M^{III}$(1,3-pdta)]·xH_2O (M = Fe [28], Ru [29-31], V [32], Cr and Rh [33]), $(PPh_4)_4[(W_3SO_3)_2$(1,3-

pdta)$_3$]·39H_2O [34], and insoluble coordination polymer $(NH_4)_{8n}[Mo_{10}O_{32}(1,3\text{-pdta})]_n$·30n$H_2O$.[35] Comparing with transition metals, lanthanide ions have high coordination number (CN) and coordination flexibility. Involving ethylenediaminetetraacetate lanthanide complexes, they often form monomeric complexes as transition metal complexes [36]. Unlike most of the monomeric propanediaminetetraacetato transition metal complexes, propanediaminetetraacetato lanthanides form dimeric $M[Ln_2(pdta)_2(H_2O)_4]$ or polymeric complexes $M'[Ln(pdta)(H_2O)]_n$ [37-46]. This may come from the coordination versatility and flexibility of pdta ligand. Combination of these might be expected to isolate different sorts of lanthanide complexes, which are also important precursors in sol-gel processing [47, 48].

Previously, we have reported some lanthanide pdta complexes used as the precursors of catalysts for the oxidative coupling of methane [49]. Herein, in acidic solution, five types of 1,3-propanediaminetetraacetato lanthanides were isolated and fully characterized with the increments of pH value and reaction temperature: 1D-CPs $[Ln(1,3\text{-}H_3pdta)(H_2O)_5]_n\cdot Cl_{2n}\cdot 3nH_2O$ [Ln = La, **1**; Ce, **2**; Pr, **3**; Nd, **4**; Sm, **5**] for type *a*, 1D-CPs $[Ln(1,3\text{-}H_2pdta)(H_2O)_3]_n\cdot Cl_n\cdot 2nH_2O$ [Ln = Sm, **6**; Gd, **7**] for type *b*, 2D-CPs $[Ln(1,3\text{-}H_2pdta)(H_2O)_2]_n\cdot Cl_n\cdot 2nH_2O$ [Ln = La, **8**; Ce, **9**; Pr, **10**; Nd, **11**; Sm, **12**; Eu, **13**; Gd, **14**] were isolated at 70 °C for type *c*, 3D-CPs $[Ln(1,3\text{-Hpdta})]_n\cdot nH_2O$ [Ln = La, **15**; Ce, **16**; Pr, **17**; Nd, **18**] for type *d*, and samarium and europium complexes were isolated as 2D-CPs $[Ln(1,3\text{-Hpdta})(H_2O)]_n\cdot 4nH_2O$ (Sm, **19**; Eu, **20**) for type *e*. The former is used as a catalyst for the ester hydrolysis.

2. Experimental

2.1 Synthesis

*2.1.1 Preparation of $[La(1,3\text{-}H_3pdta)(H_2O)_4]_n\cdot 2Cl_n\cdot 3nH_2O$ (**1**).*

KOH (1.12 g, 20.0 mmol) and 1,3-propanediaminetetraacetic acid (6.2 g, 20.0 mmol) were dissolved in water (75 mL) and stirred for several minutes. $LaCl_3 \cdot 7H_2O$ (7.4 g, 20.0 mmol) was added. The pH value was 1.5-2.0. The solution was stirred for half an hour and then standing in air. Colorless crystalline materials were separated after evaporation of the solution. The solids were washed with cold water and ethanol, and dried in the air. The yield of **1** was 92% (12.1 g). Anal. Found (calcd. for $C_{11}H_{33}N_2O_{16}Cl_2La$): C, 19.7 (20.0); H, 5.1 (5.0); N, 4.0 (4.2). IR (KBr disk, /cm^{-1}): 3404_s, 3019_s, $\nu_{as}(CO_2H)$, 1739_s, 1707_s, $\nu_{as}(CO_2)$, 1616_s; $\nu_s(CO_2)$, 1413_s; 1342_m, 1254_m, 1197_m, 1119_w, 1067_m, 971_w, 907_w, 883_m, 851_w, 700_m, 533_w, 477_w. Solution ^{1}H NMR (500 MHz, D_2O): δ (ppm) 3.993 (8H, s), 3.446 (4H, t, J = 7.5 Hz), 2.242 (2H, m); ^{13}C NMR (500 MHz, D_2O): δ (ppm) 172.7 (−**C**O_2), 59.6 (−**C**H_2CO_2), 56.0 (−N**C**H_2−), 22.4 (−**C**H_2−). Solubility in water at 25 °C (~ 0.6 g·mL^{-1}). Preparations of **2** ~ **5** were similar to that of **1**.

*2.1.2 Preparation of $[La(1,3\text{-}H_2pdta)(H_2O)_2]_n \cdot Cl_n \cdot 2nH_2O$ (**8**).*

KOH (0.11 g, 2.0 mmol) and crystal or powder of $[La(1,3\text{-}H_3pdta)(H_2O)_4]_n \cdot Cl_{2n} \cdot 3nH_2O$ (**1**) (1.32 g, 2.0 mmol) were dissolved in water (15 mL) and stirred for half an hour and then standing in 70 °C. The pH value was 2.6-3.1. Colorless crystalline materials were separated after evaporation of the solution. The solids were washed with water and ethanol, and dried in the air. The yield of **8** was 81% (0.89 g). Anal. Found (calcd. for $C_{11}H_{24}N_2O_{12}ClLa$): C, 23.8 (24.0); H, 4.5 (4.4); N, 5.0 (5.1). IR (KBr disk, /cm^{-1}): 3590_s, 3442_{vs}, 3396_{vs}, 3315_{vs}, 3176_{vs}, 3138_{vs}, 3044_{vs}, 3022_{vs}, 2999_{vs}, $\nu_{as}(CO_2)$, 1670_s, 1643_{vs}, 1617_{vs}; $\nu_s(CO_2)$, 1471_w, 1444_s, 1434_s, 1412_{vs}, 1397_{vs}, 1348_s; 1270_w, 1251_m, 1233_m, 1211_m, 1113_w, 1058_m, 1035_m, 996_w, 958_m, 904_m, 867_m, 847_w, 727_m, 693_m, 660_m, 593_m, 565_w, 517_w, 498_w. Preparations of complexes **9**-**12** were similar to that of **8**. Owing to the unsuccessful isolation of type a complexes for europium and gadolinium, complexes **13** and **14** were isolated only through one pot synthesis process. KOH (0.22 g, 4.0 mmol) and 1,3-propanediaminetetraacetic acid (0.62 g, 2.0 mmol) were added in water (15 mL) and stirred for

several minutes, then $EuCl_3 \cdot 7H_2O$ (0.74 g, 2.0 mmol) was added. The solution was stirred for half an hour and then standing in 70 °C. Colorless crystalline materials were separated after evaporation of the solution. The solids were washed with water and ethanol, and dried in the air. The yield of **13** was 78% (0.88 g). Anal. Found (calcd. for $C_{11}H_{24}N_2O_{12}ClEu$): C, 23.5 (23.4); H, 4.5 (4.3); N, 5.1 (5.0). IR (KBr disk, /cm^{-1}): 3583_s, 3441_{vs}, 3331_{vs}, 3181_{vs}, 3125_{vs}, 3051_{vs}, $\nu_{as}(CO_2)$, 1677_s, 1618_{vs}; $\nu_s(CO_2)$, 1399_{vs}, 1350_s, 1309_{vs};, 1236_m, 1212_m, 1114_w, 1059_m, 1036_m, 999_w, 964_m, 906_m, 871_m, 725_m, 693_m, 596_m, 567_w, 523_w, 499_w, 414_w. Preparations of **14** were similar to that of **13**.

*2.1.3 Synthesis of $[La(1,3\text{-}Hpdta)]_n \cdot nH_2O$ (**15**).*

KOH (0.06-0.11 g, 1.0-2.0 mmol), water (15 mL) and crystal or powder of $[La(1,3\text{-}H_3pdta)(H_2O)_4]_n \cdot Cl_{2n} \cdot 3nH_2O$ (**1**) (1.32 g, 2.0 mmol) were sealed into a 25 mL teflon-lined stainless steel vessel, heated at 180 °C for 60 h, and then slowly (40 h) cooled to room temperature. Colorless crystalline materials were separated. The solids were washed with water, and dried in the air. The yield of **15** was 65% (0.30 g). Anal. Found (calcd. for $C_{11}H_{17}N_2O_9La$): C, 28.8 (28.7); H, 3.9 (3.7); N, 6.1 (6.1). IR (KBr disk, /cm^{-1}): 3481_m, 3447_m, 3126_m, 3019_w, 3002_w, 2969_w, 2899_w, 2883_w, $\nu_{as}(CO_2)$, 1665_s, 1636_{vs}, 1614_{vs}, 1599_{vs}; $\nu_s(CO_2)$, 1480_w, 1401_{vs}, 1385_{vs}, 1334_s, 1321_m; 1296_w, 1271_w, 1254_w, 1232_m, 1161_w, 1125_w, 1090_w, 1066_w, 1031_w, 994_w, 980_w, 916_w, 878_m, 864_m, 759_w, 738_m, 718_m, 615_m, 595_m, 551_w, 541_w, 484_w. Preparations of complexes **16**-**19** were similar to that of **15**.

*2.1.4 One pot synthesis of $[La(1,3\text{-}H_2pdta)(H_2O)_2]_n \cdot Cl_n \cdot 2nH_2O$ (**8**).*

KOH (0.22 g, 4.0 mmol) and 1,3-propanediaminetetraacetic acid (0.62 g, 2.0 mmol) were dissolved in water (15 mL). $LaCl_3 \cdot 7H_2O$ (0.74 g, 2.0 mmol) was added. The solution was stirred for half an hour and then standing in 70 °C. Colorless crystalline materials were separated after evaporation of the solution. The solids were washed with water and ethanol, and dried in the air.

The yield of **8** was 75% (0.83 g). Anal. Found (calcd. for $C_{11}H_{24}N_2O_{12}ClLa$): C, 23.8 (24.0); H, 4.5 (4.4); N, 5.0 (5.1). One pot synthesis of complexes **9-14** were similar to that of **8**. Synthesis of $[Ln(1,3\text{-}H_2pdta)(H_2O)_3]_n{\cdot}Cl_n{\cdot}2nH_2O$ [Ln = Sm, **6**; Gd, **7**] were similar to that of **8**, but standing in room temperature**.**

*2.1.5 One pot synthesis of $[La(1,3\text{-}Hpdta)]_n{\cdot}nH_2O$ (**15**).*

KOH (0.11-0.17 g, 2.0-3.0 mmol), 1,3-propanediaminetetraacetic acid (0.31 g, 1.0 mmol), water (15 mL) and $LaCl_3{\cdot}7H_2O$ (0.37 g, 1.0 mmol) were sealed into a 25 mL teflon-lined stainless steel vessel, heated at 180 °C for 60 h, and then (40 h) cooled to room temperature. Colorless crystalline materials were separated. The solids were washed with water, and dried in air. The yield of **15** was 55% (0.25 g). Anal. Found (calcd. for $C_{11}H_{17}N_2O_9La$): C, 28.8 (28.7); H, 3.9 (3.7); N, 6.1 (6.1). One pot synthesis of complexes **16-20** were similar to that of **15**.

2.2 X-ray diffraction data

Suitable single crystals of **1-20** were selected and quickly mounted onto thin glass fibers to prevent the loss of water molecules. X-ray diffraction data were measured at 173 K on an Oxford CCD diffractometer with Mo Kα radiation (λ = 0.71073 Å). Empirical adsorption was applied to all data using SADABS and CrysAlis (multi-scan) program. The initial model was obtained through direct methods and the completion of the rest of the structure achieved by difference Fourier strategies. The structures were refined by least squares on F^2, with anisotropic displacement parameters for non-H atoms. All calculations to solve and refine the structures and to obtain the derived results were carried out with the computer programs SHELXS 97, and SHELXL 97 programs.[50, 51] CCDC deposition numbers are 967707-967717 and 967719-967727. Crystal data and structures refinements for **1-20** are summarized in Table S1-S3.

2.3 Physical measurements

All chemicals were of analytical or reagent-grade purity and used as received. The pH value was measured by potentiometric method with a PHB-8 digital pH meter. Elemental analyses (C, H, N) were performed by EA1110 elemental analyzer. Solution ^{13}C and ^{1}H NMR spectra were recorded in D_2O on a Bruker AV 500 M NMR spectrometer using DSS (sodium 2,2-dimethyl-2-silapentane-5-sulfonate) as the internal reference. A Bruker esquire 3000plus instrument was used to record the Electrospray ionization (ESI) mass spectra. Infrared spectra were recorded as KBr disks and as mulls in Nujol with a Nicolet 330 FT-IR spectrophotometer. Thermogravimetric analysis were recorded on SDT-Q600 thermal analyzer, under an air flow of 100 $ml \cdot min^{-1}$ at a heating rate of 10 $°C \cdot min^{-1}$. Luminescent spectra were recorded on Hitachi F7000 spectrometer.

3. Results and discussion

3.1 Synthesis

Previously, it is reported that reactions of lanthanide salts with pdta result in the coordination of nitrogen atoms and oxygens of pdta [37-46]. While isolation of water-soluble coordination polymer shows that nitrogen atoms do not coordinate with lanthanide ions and could be transformed to the other species in this report as shown in Scheme 1. The synthesis of $[Ln(1,3\text{-}H_3pdta)(H_2O)_5]_n \cdot Cl_{2n} \cdot 3nH_2O$ (**1-5**) were carried out in strong acidic aqueous solutions. Combinations of $LnCl_3/H_4pdta/KOH$ in molar ratio of 1 : 1 : 1 resulted in the formation of soluble 1D-CPs (type a) with a high yield of 92% for lanthanum complex **1**. When more potassium hydroxide were added into their solution to adjust the pH value to 2.6-3.1, two new 1D-CPs $[Ln(1,3\text{-}H_2pdta)(H_2O)_3]_n \cdot Cl_n \cdot 2nH_2O$ [Ln = Sm, **6**; Gd, **7**] (type b) were isolated at room temperature and seven 2D-CPs $[Ln(1,3\text{-}H_2pdta)(H_2O)_2]_n \cdot Cl_n \cdot 2nH_2O$ (**8-14**) (type c) were isolated at 70 °C. When crystals of **1**−**4** were heated at 180 °C with 1-2 eq. potassium hydroxide, four 3D

coordination polymers $[Ln(1,3\text{-}Hpdta)]_n \cdot nH_2O$ [Ln = La, **15**; Ce, **16**; Pr, **17**; Nd, **18**] (type d). Two 2D coordination polymer $[Ln(1,3\text{-}Hpdta)(H_2O)]_n \cdot 4nH_2O$ (Sm, **19**; Eu, **20**) (type e) were isolated in similar condition. Moreover, as shown in Scheme 1, complexes type b and c can be directly transformed to type d and e complexes. The yields are high (90-95 %) for type d and e complexes in this method. We found that in moderate acidic solution, lanthanide complexes show little lanthanide contraction effect at moderate temperature. But in strong acidic solution, there exist obvious difference that makes the isolation of similar complexes of europium and gadolinium difficult. In high temperature, there show lanthanide contraction effect that makes complexes **19** and **20** show different structure with complexes **15-18** in similar reaction conditions, which has found in some systems like 3-aminopyrazine-2-carboxylic acid and isonicotinate-N-oxide lanthanide system [13, 52-54].

[Scheme 1]

3.2 Crystal structures analysis

X-ray structure analysis revealed that $[La(1,3\text{-}H_3pdta)(H_2O)_5]_n \cdot Cl_{2n} \cdot 3nH_2O$ (**1**) is a zonal coordination polymer with mononuclear subunit $[La(1,3\text{-}H_3pdta)(H_2O)_5]$ as shown in Figure 1. In an asymmetric unit, La(III) cation exists in nonadentate coordination environment, which contains four carboxy oxygen atoms and five water molecules. H_3pdta uses its two carboxy oxygen atom bonded to different nitrogen atoms to chelate one lanthanum ions, forming a twelve membered ring, and still uses its other two carboxy oxygen atoms to coordinate with other two lanthanum ions, forming a 1D-CP structure as shown in Figure 2. The 1D- CP structure was extended to a 3D supramolecular structure through hydrogen bonds between water molecules and Cl^-. It is interesting to note that in **1** there is a very strong intramolecular hydrogen bond [O4···O8 2.398(9) Å, $x + 1, + y, z + 1$]. The molecular structures of **2-5** are isomorphous with that of **1**, as shown in Figures S1-S4.

[Figures 1 and 2]

$[Sm(1,3\text{-}H_2pdta)(H_2O)_3]_n \cdot Cl_n \cdot 2nH_2O$ (**6**) is also a 1D-CP. In an asymmetric unit, Sm(III) cation exists in nonadentate coordination environment, which contains six carboxy oxygen atoms from three different H_2pdta and three water molecules as shown in Figure 3. H_2pdta uses its two carboxy groups bonded to different nitrogen atoms to chelate with one Sm(III) cation, one forming a four membered chelated ring with Sm^{3+}. It still uses its other two carboxy groups to coordinate and chelate with other two Sm^{3+}. This makes it form an infinite 1D-CP as shown in Figure 4. The structure of **7** is similar to that of **6** as shown in Figure S5.

[Figures 3 and 4]

$[La(1,3\text{-}H_2pdta)(H_2O)_2]_n \cdot Cl_n \cdot 2nH_2O$ (**8**) is a 2D-CP. In an asymmetric unit, La(III) cation exists in octadentate coordination environment, which contains six carboxy oxygen atoms from four different H_2pdta and two water molecules as shown in Figure 5. Comparing the formula of **8** with **6**, there is only one less coordination water molecule in **8**, but there exist big difference in structures. H_2pdta uses its two carboxy groups bonded to different nitrogen atoms to coordinate with one La(III) cation, one still use its other carboxy oxygen atom to coordinate with another La(III) cation. It still uses its other two carboxy groups to coordinate and chelate with other three La^{3+}. This makes it form an infinite 2D-CP as shown in Figure 6. The structures of **9-14** are similar to that of **8** as shown in Figures S6-S11.

[Figures 5 and 6]

X-ray structure analysis revealed that $[La(1,3\text{-}Hpdta)]_n \cdot nH_2O$ (**15**) is a 3D-CP with neutral mononuclear subunit $[La(1,3\text{-}Hpdta)]_n$ and one crystal water molecules, as shown in Figures 7 and 8. In an asymmetric unit, La(III) cation exists in nonadentate coordination environment, which contains eight carboxy oxygen atoms from six different Hpdta ligands and one nitrogen

atom. These Hpdta ligands make the compound be a 3D-CP. The structures of **16-18** are similar to that of **15** as shown in Figures S12-S14.

[Figures 7 and 8]

The crystal structure of **19** consists of a dimeric neutral unit $[Sm_2(Hpdta)_2(H_2O)_2]_n$ and eight crystallized water molecules, as shown in Figure 9. Samarium ion is octa-coordinated, Sm1 is surrounded by six oxygen atoms from four different trident acetates of Hpdta anion, one nitrogen and one water molecule. Two chelated rings are formed by nitrogen and oxygen atoms of Hpdta, which further couples with the other carboxy group of Hpdta into a dimeric unit. For the structures of **19**, the dimeric units further connected by the oxygen atoms of carboxy groups to generate infinite 2D layered structures respectively as shown in Figure 9, and forms 3D supramolecular structures by intermolecular hydrogen bonds. The molecular structure of **20** is similar to **19**, as shown in Figure S15.

[Figure 9]

Table 1. Selected bond lengths (Å), coordination number (C.N.) of lanthanide and dentate number (D.N.) of pdta ligands for **1-20**.

Entry	Ln-$O_{carboxy}$(av)	Ln–N	Ln–Ow (av)	C.N.	D.N.
1-La	2.562(5)	-	2.566(5)	9	4
2-Ce	2.541(4)	-	2.537(4)	9	4
3-Pr	2.528(4)	-	2.526(5)	9	4
4-Nd	2.522(7)	-	2.513(7)	9	4
5-Sm	2.493(3)	-	2.488(3)	9	4
6-Sm	2.488(4)	-	2.445(4)	9	6
7-Gd	2.461(3)	-	2.417(3)	9	6
8-La	2.505(2)	-	2.553(2)	8	6
9-Ce	2.478(2)	-	2.523(2)	8	6
10-Pr	2.460(2)	-	2.505(2)	8	6
11-Nd	2.447(2)	-	2.491(2)	8	6
12-Sm	2.416(2)	-	2.464(2)	8	6
13-Eu	2.407(2)	-	2.445(2)	8	6
14-Gd	2.392(2)	-	2.432(2)	8	6
15-La	2.571(4)	2.858(3)	-	9	9
16-Ce	2.552(5)	2.825(3)	-	9	9
17-Pr	2.553(6)	2.798(4)	-	9	9
18-Nd	2.523(3)	2.780(2)	-	9	9
19-Sm	2.481(5)	2.711(5)	2.450(6)	8	7
20-Eu	2.471(5)	2.692(5)	2.441(5)	8	7

Selected bond lengths (Å), coordination number (C.N.) of lanthanide and dentate number (D.N.) of pdta ligands for **1-20** were shown in Table 1. From the table, we found obvious lanthanide contraction effect. The bond distances decreases with the increases of lanthanide number. The coordination number (C.N.) of lanthanide shows little relationship with lanthanide

number, but the temperature and pH values will affect the C.N. of lanthanide. The C.N. of complexes **8-14** and **19** and **20** is eight, while the others are nine. Comparing the C.N. of **15-18** with **19** and **20**, obviously, this C.N. differences come from the lanthanide contraction effects. We also found out that the number of coordinate water molecules decreases and the dentate number of pdta increases with the increases of pH values.

3.3 Solution analysis

Solution ^{13}C NMR spectra of **1** and H_4pdta are showed in Figure 10. Solution ^{1}H NMR spectra are listed in Figures S16 ~ S17. Comparing ^{13}C NMR spectrum of **1** with that of H_4pdta, there exist small downfield shift. Moreover, it is the fact that two kinds of carboxy carbon in **1** give only one set of ^{13}C NMR signal at 172.7 ppm ($\Delta\delta = 0.8$ ppm) and one $-\mathbf{C}H_2CO_2$ signal at 59.6 ppm ($\Delta\delta = 0.8$ ppm). For the $\Delta\delta$ is quite small, we cannot make sure the coordination state in aqueous state. But these can indicate the less strongly bounded carboxy group get the same chemical environment with the other carboxy groups that bounded to the same nitrogen in **1**. There is also only one set signal of $-CH_2N-$ (56.0 ppm, $\Delta\delta = 0.2$ ppm) and $-CH_2N-$ (22.4 ppm, $\Delta\delta = 0.2$ ppm) in **1**. For the better understanding of its solution state, the ion signals of the water solution mass spectra for **1** were measured in the positive ionization (negative mode show very little signal) mode by ESI. As shown in Fig. S18, compound **1** exhibited three strong peaks at 130.5, 253.1 and 446.7 m/z, the corresponding calculated unit is not very clear. But we can make sure that the 446.7 m/z is bigger than that of $[La(1,3\text{-}H_2pdta)]^+$ (m/z = 443.2) and may correspond to $[La_5(1,3\text{-}H_2pdta)_5H_2O]^{5+}$ (m/z = 446.8). Then we detected the mass spectra in methanol and water solution (CH_3OH: H_2O = 2:1). As shown in Fig. S19, the three strong peaks also existed, but another peak at 575.4 m/z grown a lot. The new strong peak may correspond to the dimeric unit. This indicate compound **1** in solution state may exist in aggregate state in a certain

percentage, and in water solution, the aggregate state is less than in a mixed methanol-water solution. This is consistent with the solution ^{13}C NMR analysis.

In ^{1}H NMR spectrum of H_4pdta (Fig. S16), the eight acetate protons are equivalent and result in one signal at 4.061 ppm. The four $–CH_2N–$ protons are equivalent and result in a triple signal centred at 3.433 ppm, and the two protons of $–CH_2–$ give a penta-signal centred at 2.249 ppm. When we compare the ^{1}H NMR spectra of H_4pdta and lanthanum complex **1** (Fig. S17), we find out that they give only one set of signal which is consistent with the ^{13}C NMR spectra. Through the ^{1}H NMR spectrum of **1**, we can find a singlet at 3.993 ppm (8H, s, $\Delta\delta$ = –0.068 ppm) for acetate protons and a tri-signal centred at 3.446 ppm (4H, t, J = 7.5 Hz, $\Delta\delta$ = 0.033 ppm) for the $–CH_2N–$ protons and multiple peaks centred at 2.242 (2H, m, $\Delta\delta$ = –0.007 ppm). There are small $\Delta\delta$ for **1**. This is an indication for the weak coordination of propanediaminetetraacetate in **1**.

[Figure 10]

3.4 IR spectra analysis

IR vibrational spectra of **1-20** are listed in Figures S20-S22. In the region between 1630 and 1540 cm^{-1} and between 1450 and 1320 cm^{-1}, compounds **1-20** give two typical bands that correspond to the bounded carboxy group $\nu_{as}(COO^-)$ and $\nu_s(COO^-)$, respectively. In complexes **1-5**, there are protonated carboxy groups and give an absorption peak around 1709 cm^{-1}. The value of $[\nu(COO^-)_{as} - \nu(COO^-)_s]$ is about 203 cm^{-1} in **1** suggests that the monodentate coordination of the carboxy groups. These changes confirm that the oxygen atoms from the carboxy groups of pdta have coordinated with the centre ions.[55] A broad ν(OH) band near 3404 cm^{-1} indicates H_2O in the complex **1-5**. The ν(C−N) of complexes **1** at 1067 cm^{-1} displays no obvious shift compared with that of H_4pdta (1068 cm^{-1}), suggesting that nitrogen atoms of pdta are not coordinated to lanthanum. These are also observed for **2-14**. The ν(C−N) of complexes **15-20** display two bands

around 1100 cm^{-1}, one displays obvious blue-shift compared with that of H_4pdta, suggesting that one nitrogen atom of pdta coordinate with the centre ions.

3.5 Thermogravimetric analysis

Thermal stability and decomposition patterns of the complexes were investigated by thermo-gravimetric analyses. The TG-DTG curves are listed in Figures S23-S42. As shown in Figure 11, the first part of big weight losses of **1** at 110 °C corresponds to the loss of crystal water molecules and one hydrogen chloride. Then some coordinated water molecules lose at 218 °C. The ligand may decompose from 286 to 461 °C. The final residue of compound **1** is LaOCl. Comparing the TG curves of lanthanum compounds **1** (type a), **8** (type c) and **15** (type d), we found out that acidic condition is helpful to get oxides at a lower temperature. Similar results can be found in the other lanthanide compounds of these three types of lanthanide compounds. The remainder four compounds of type b and type e didn't show this feature.

[Figure 11]

3.6 Luminescent spectra analysis

Figure 12 shows the luminescent spectra of the obtained europium polymers **13** and **20**. Four curves represent the spectra of excitation and emission spectra of **13** (blue and black curves) and **20** (red and violet curves), respectively. The excitation spectra are obtained by monitoring the emission of europium polymers at 595 or 615 nm. For excitation spectra of these two polymers, eight absorption bands are found in the range of 315–470 nm, suggesting the effective absorption of the hybrid systems. And these two polymers show similar excitation spectra. Therefore, in order to compare the emission spectra of these two hybrid materials under the same conditions, they should be monitored using the same and the most appropriate excitation wavelength (394 nm). As a result, the emission lines of the polymeric hybrid materials are obtained from the $^5D_0$–

^7F_J (J = 0–4) transitions at about 580, 590, 595, 614, 618, 652 nm for **13** and 580, 587, 596, 615, 625 and 652 nm for **20**. Among these emission peaks of **20**, the most striking red fluorescence signals ($^5D_0$–$^7F_2$) of the induced electric dipole transition at about 615 nm is stronger than the orange emission intensities of the magnetic dipole transition $^5D_0$–$^7F_1$ at about 596 nm, which indicates an Eu3+ site in an environment without inversion symmetry.[56-58] While for polymer **13**, they show different emission spectra with **20**, the most striking fluorescence signals is the magnetic dipole transition $^5D_0$–$^7F_1$ at about 595 nm, and the induced electric dipole transition at about ($^5D_0$–$^7F_2$) 618 nm is a little weaker than the orange emission intensities at 595 nm. As can be seen from the spectra, these two polymers show a different ratio of red/orange, which indicated that they have a different coordination environment. This is consistent with structure analysis. Furthermore, we compared the relative luminescent intensities of these two europium polymers. To ensure the accuracy of comparison and prevent insufficient absorption of the exciting radiation, a powder layer around 2 mm was used and utmost care was taken in order to ensure that only the sample was illuminated and the measurements were under the same conditions. Then we found the relative intensity of **20** is stronger than that of **13**.

[Figure 12]

3.7 Catalytic activity for ester hydrolysis reaction

In a typical experiment, four test tubes with 4.0 mL water solution were tested for the catalytic esterification. The solution contains 1.0 mmol catalysts of [La(1,3-H_3pdta)$(H_2O)_5]_n$·$2Cl_n$·$3nH_2O$ (**1**), [Sm(1,3-H_3pdta)$(H_2O)_5]_n$·$2Cl_n$·$3nH_2O$ (**5**), KH_3pdta and $LaCl_3$, respectively. Each tube was added with one drop of 0.1 mol·L^{-1} methyl orange for the clarity of observation. Then 1.0 mL ethyl acetate (~10 mmol) was added to the above solution respectively, and the catalytic reaction temperature was maintained at 70 ^oC. The height of the upper solution was measured every 15 minutes as shown in Table 2. Water-soluble coordination polymer**s 1** and

5 can hydrolyze ethyl acetate with a certain speed. This is because that both of the lanthanides have weak acid properties in solution. It seems that samarium propanediaminetetraacetate **5** gives little better catalytic activity than that of lanthanum propanediaminetetraacetate **1**, which is attributed to the lanthanide contraction and the decrease of basicity in samarium catalyst. Moreover, ethyl acetate shows no hydrolysis by the independent ligand of KH_3pdta or $LaCl_3$ salt as a blank sample. Synergistic effects of lanthanide and the ligand may play an important role in the catalytic reaction of ester hydrolysis. In another word, the ester hydrolysis was catalyzed by hydrogen 1,3-propanediaminetetraacetato lanthanide, which is interesting result for the ester hydrolysis by water-soluble coordination polymer.

Table 2. The height of the ethyl acetate in every 15 minutes.[a]

	0 min	15.0 min	30.0 min
1	9.0 mm	7.0 mm	5.9 mm
5	9.0 mm	7.0 mm	5.7 mm
KH_3pdta	9.0 mm	9.0 mm	9.0 mm
$LaCl_3$	9.0 mm	9.0 mm	9.0 mm

[a] When ethyl acetate was hydrolyzed, the products of acetic acid and ethanol can be dissolved in aqueous phase which contains methyl orange. Thus, the height of organic phase for ethyl acetate can be observed easily and decreased with the hydrolyzed process.

4. Conclusions

In summary, novel rare-earth coordination polymers possessing different types of structures for 1,3-propanediaminetetraacetatic acid have been successfully isolated under acidic conditions, which exhibit water-soluble 1D-CPs LnH_3pdta (La, Ce, Pr, Nd, Sm) and 1D-CPs LnH_2pdta (Sm, Gd), 2D-CPs LnH_2pdta (La, Ce, Pr, Nd, Sm, Eu, Gd) and LnHpdta (Sm, Eu), as well as 3D-CPs LnHpdta (La, Ce, Pr, Nd). The structure diversity is mainly caused by the variation of coordinated ligand and lanthanide contraction effect. The thermal stability investigations reveal that acidic

condition is helpful to get oxides at lower temperature. The successful synthesis of the twenty complexes provides a valuable approach for the construction of rare-earth coordination polymers tuned by pH value, temperature and lanthanide contraction effect. Moreover, the catalytic activities of **1** and **5** to ester hydrolysis and the luminescent spectra of europium polymers **13** and **20** were also researched. Efforts to further systematic studies for these and other lanthanide complexes are ongoing.

Acknowledgements

This work was financially supported by the National Science Foundation of China and the Ministry of Science and Technology of China (2010CB732303) and PCSIRT (No. IRT1036).

Appendix A. Supplementary data

† ABBREVIATIONS: 1,3-H_4pdta, 1,3-propanediaminetetraacetatic acid $CH_2[CH_2N(CH_2CO_2H)_2]_2$; 1D-CP, one dimensional coordination polymer; 2D-CP, two dimensional coordination polymer; 3D-CP, three dimensional coordination polymer; eq., equivalent.

Electronic Supplementary Information (ESI) available: Ortep structures of the other complexes, ^{1}H NMR spectra, IR spectra, TG-DTG curves, and the X-ray crystallographic data of **1**-**20** in CIF format.

References

[1] L. Guo, B. Yan, J.L. Liu, K. Sheng, X.L. Wang, Dalton Trans. 40 (2011) 632–638.

[2] L.W. Han, J. Lü, T.F. Liu, S.Y. Gao, R. Cao, Dalton Trans. 39 (2010) 10967–10973.

[3] C. Daiguebonne, N. Kerbellec, O. Guillou, J.C. Bünzli, F. Gumy, L. Catala, T. Mallah, N. Audebrand, Y. Gérault, K. Bernot, G. Calvez, Inorg. Chem. 47 (2008) 3700–3708.

[4] Y.L. Gai, K.C. Xiong, L. Chen, Y. Bu, X.J. Li, F.L. Jiang, M.C. Hong, Inorg. Chem. 51 (2012) 13128–13137.

[5] Y. Guo, W. Dou, X. Zhou, W. Liu, W. Qin, Z. Zang, H. Zhang, D. Wang, Inorg. Chem. 48 (2009) 3581–3590.

[6] N. Kerbellec, D. Kustaryono, V. Haquin, M. Etienne, C. Daiguebonne, O. Guillou, Inorg. Chem. 48 (2009) 2837–2843.

[7] O.L. Ortiz, L.D. Ramírez, Coordination polymers and metal organic frameworks : properties, types, and applications, Nova Science Publishers, Hauppauge, N.Y., 2012.

[8] Z. Lin, R. Zou, J. Liang, W. Xia, D. Xia, Y. Wang, J. Lin, T. Hu, Q. Chen, X. Wang, Y. Zhao, A.K. Burrell, J. Mater. Chem. 22 (2012) 7813–7818.

[9] Y.P. He, Y.X. Tan, J. Zhang, Inorg. Chem., 52 (2013) 12758–12762.

[10] H. Tan, B. Liu, Y. Chen, ACS Nano 6 (2012) 10505–10511.

[11] H. He, H. Ma, D. Sun, L. Zhang, R. Wang, D. Sun, Cryst. Grow. & Des. 13 (2013) 3154–3161.

[12] S.M.F. Vilela, A.D.G. Firmino, R.F. Mendes, J.A. Fernandes, D. Ananias, A.A. Valente, H. Ott, L.D. Carlos, J. Rocha, J.P.C. Tome, F.A. Almeida Paz, Chem. Commun. 49 (2013) 6400–6402.

[13] Z.P. Deng, W. Kang, L.H. Huo, H. Zhao, S. Gao, Dalton Trans. 39 (2010) 6276–6284.

[14] H. Wei, H. Zhang, G. Jin, T. Na, G. Zhang, X. Zhang, Y. Wang, H. Sun, W. Tian, B. Yang, Adv. Funct. Mater. 23 (2013) 4035–4042.

[15] P. Smolenski, S.W. Jaros, C. Pettinari, G. Lupidi, L. Quassinti, M. Bramucci, L.A. Vitali, D. Petrelli, A. Kochel, A.M. Kirillov, Dalton Trans. 42 (2013) 6572–6581.

[16] M. Yamada, F. Hamada, Crystengcomm 15 (2013) 5703–5712.

[17] M. Fontanet, M. Rodriguez, I. Romero, X. Fontrodona, F. Teixidor, C. Vinas, N. Aliaga–Alcalde, P. Matejicek, Dalton Trans. 42 (2013) 7838–7841.

[18] A. Molnar, EDTA: Synthesis, Uses and Environmental Concerns, Nova Science Publishers, 2013.

[19] D.D. Radanovic, U. Rychlewska, M.I. Djuran, B. Warzajtis, N.S. Draskovic, D.M. Guresic, Polyhedron 23 (2004) 2183–2192.

[20] D.D. Radanovic, U. Rychlewska, M.I. Djuran, N.S. Draskovic, M.M. Vasojevic, I.M. Hodzic, D.J. Radanovic, Polyhedron 22 (2003) 2745–2753.

[21] N.S. Draskovic, M.I. Djuran, M.S. Cvijovic, D.D. Radanovic, V. Jevtovic, Transit. Metal Chem. 29 (2004) 874–879.

[22] A. Mederos, P. Gili, S. Dominguez, A. Benitez, M.S. Palacios, M. Hernandezpadilla, P. Martinzarza, M.L. Rodriguez, C. Ruizperez, F.J. Lahoz, L.A. Oro, F. Brito, J.M. Arrieta, M. Vlassi, G. Germain, Dalton Trans. (1990) 1477–1491.

[23] D.J. Radanovic, T. Ama, H. Kawaguchi, N.S. Draskovic, D.M. Ristanovic, S. Janicijevic, Bullet. Chem. Soc. Japan 74 (2001) 701–706.

[24] U. Rychlewska, D.D. Radanovic, V.S. Jevtovic, D.J. Radanovic, Polyhedron 19 (2000) 1–5.

[25] M. Hernandez-Padilla, E. Chinea, S. Dominguez, A. Mederos, M.C. Munoz, F. Lloret, Polyhedron 19 (2000) 1175–1179.

[26] U. Rychlewska, D.M. Guresic, B. Warzajtis, D.D. Radanovic, M.I. Djuran, Polyhedron 24 (2005) 2009–2016.

[27] U. Rychlewska, B. Warzajtis, D. Cvetic, D.D. Radanovic, D.M. Guresic, M.I. Djuran, Polyhedron 26 (2007) 1717–1724.

[28] R. Meier, J. Maigut, B. Kallies, N. Lehnert, F. Paulat, F.W. Heinemann, G. Zahn, M.P. Feth, H. Krautscheid, R. van Eldik, Chem. Commun. (2007) 3960–3962.

[29] M.M.T. Khan, H.C. Bajaj, Z. Shirin, K. Venkatasubramanian, Polyhedron 11 (1992) 1059–1066.

[30] M.M.T. Khan, D. Chatterjee, R.R. Merchant, P. Paul, S.H.R. Abdi, D. Srinivas, M.R.H. Siddiqui, M.A. Moiz, M.M. Bhadbhade, K. Venkatasubramanian, Inorg. Chem. 31 (1992) 2711–2718.

[31] X.L. Hong, H. Li, C.H. Peng, J. Mol. Struct. 990 (2011) 197–203.

[32] J.C. Robles, Y. Matsuzaka, S. Inomata, M. Shimoi, W. Mori, H. Ogino, Inorg. Chem. 32 (1993) 13–17.

[33] R. Herak, G. Srdanov, M.I. Djuran, D.J. Radanovic, M. Bruvo, Inorg. Chim. Acta 83 (1984) 55–64.

[34] S.B. Yu, M. Droege, S. Downey, B. Segal, W. Newcomb, T. Sanderson, S. Crofts, S. Suravajjala, E. Bacon, W. Earley, D. Delecki, A.D. Watson, Inorg. Chem. 40 (2001) 1576–1581.

[35] G.G. Gao, L. Xu, X.S. Qu, H. Liu, Y.Y. Yang, Inorg. Chem. 47 (2008) 3402–3407.

[36] N. Sakagami, Y. Yamada, T. Konno, K. Okamoto, Inorg. Chim. Acta 288 (1999) 7–16.

[37] X. Chen, D. Li, J. Wang, B. Liu, Y. Kong, D. Wang, X. Zhang, J. Coord. Chem. 63 (2010) 3897–3906.

[38] N. Graeppi, D.H. Powell, G. Laurenczy, L. Zekany, A.E. Merbach, Inorg. Chim. Acta 235 (1995) 311–326.

[39] B. Liu, P. Hu, J. Wang, R. Xu, L.Q. Zhang, J. Gao, Y.F. Wang, X.D. Zhang, Russ. J. Coord. Chem. 35 (2009) 758–765.

[40] P. Thakur, J.L. Conca, G.R. Choppin, J. Coord. Chem. 64 (2011) 3215–3237.

[41] J. Wang, G.R. Gao, Z.H. Zhang, X.D. Zhang, X.Z. Liu, Y.M. Kong, Y. Li, J. Coord. Chem. 59 (2006) 2113–2123.

[42] J. Wang, P. Hu, G. Han, L. Zhang, D. Li, R. Xu, X. Chen, X.D. Zhang, J. Struct. Chem. 52 (2011) 575–581.

[43] J. Wang, P. Hu, B. Liu, X. Chen, L.Q. Zhang, G.X. Han, R. Xu, X.D. Zhang, Russ. J. Inorg. Chem. 55 (2010) 1567–1573.

[44] J. Wang, P. Hu, B. Liu, R. Xu, X. Wang, D. Wang, L.Q. Zhang, X.D. Zhang, J. Struct. Chem. 52 (2011) 568–574.

[45] J. Wang, P. Hu, B. Liu, R. Xu, X. Wang, L. Xu, L.Q. Zhang, X.D. Zhang, Russ. J. Coord. Chem. 36 (2010) 66–72.

[46] J. Wang, D. Li, J. Gao, B. Liu, B. Wang, D. Wang, T. Fan, X. Zhang, J. Coord. Chem. 63 (2010) 3792–3804.

[47] Q.M. Wang, B. Yan, J. Photochem. Photobiology A-Chem. 178 (2006) 70–75.

[48] W. Zhou, Y.H. Zheng, G.H. Wu, Applied Surface Science 253 (2006) 1387–1392.

[49] M.L. Chen, Y.H. Hou, W.S. Xia, W.Z. Weng, Z.X. Cao, Z.H. Zhou, H.L. Wan, Dalton Trans. 43 (2014) 8690–8697.

[50] A.J.C. Wilson, International Tables for Crystallography, 1995.

[51] G.M. Sheldrick, SHELXS-97, SHELXL-97, and SHELXTL/PC, Programs for solution and refinement of crystal structures, University of Göttingen, Göttingen, 1997.

[52] Z. He, E.Q. Gao, Z.M. Wang, C.H. Yan, M. Kurmoo, Inorg. Chem. 44 (2005) 862–874.

[53] J. Xia, B. Zhao, H.S. Wang, W. Shi, Y. Ma, H.B. Song, P. Cheng, D.Z. Liao, S.P. Yan, Inorg. Chem. 46 (2007) 3450–3458.

[54] Q.Y. Liu, L. Xu, Eur. J. Inorg. Chem. 2005 (2005) 3458–3466.

[55] K. Nakamoto, Infrared and Raman Spectra of Inorganic and Coordination Compounds: Part B., Applications in Coordination, Organometallic, and BioInorganic Chemistry, John Wiley & Sons, Inc., New Jersey, 2009.

[56] S. Surble, C. Serre, F. Millange, F. Pelle, G. Ferey, Solid State Sci. 9 (2007) 131–136.

[57] Y. Hasegawa, M. Yamamuro, Y. Wada, N. Kanehisa, Y. Kai, S. Yanagida, J. Phys. Chem. A 107 (2003) 1697–1702.

[58] A.F. Kirby, D. Foster, F.S. Richardson, Chem. Phys. Lett. 95 (1983) 507–512.

Figure legends

Scheme 1. Synthesis and conversions of five types of acidic lanthanide pdta coordination polymers.

Figure 1. Ortep cation structure of $[La(1,3\text{-}H_3pdta)(H_2O)_5]_n{\cdot}2Cl_n{\cdot}3nH_2O$ (**1**) in 30% thermal ellipsoids.

Figure 2. The infinite 1D acidic zonal coordination structure of $[La(1,3\text{-}H_3pdta)(H_2O)_5]_n{\cdot}Cl_{2n}{\cdot}3nH_2O$ (**1**).

Figure 3. Ortep structure of dimeric cation $[Sm_2(H_2pdta)_2(H_2O)_6]^{2+}{}_n$ of $[Sm(H_2pdta)(H_2O)_3]_n{\cdot}Cl_n{\cdot}2nH_2O$ (**6**) in 30% thermal ellipsoids.

Figure 4. The infinite 1D structure of $[Sm(H_2pdta)(H_2O)_3]_n{\cdot}Cl_n{\cdot}2nH_2O$ (**6**).

Figure 5. Structure of dimeric cation $[La_2(H_2pdta)_2(H_2O)_4]^{2+}{}_n$ of $[La(H_2pdta)(H_2O)_2]_n{\cdot}Cl_n{\cdot}2nH_2O$ (**8**) in 30% thermal ellipsoids.

Figure 6. The infinite 2D structure of $[La(H_2pdta)(H_2O)_2]_n{\cdot}Cl_n{\cdot}2nH_2O$ (**8**).

Figure 7. Ortep neutral mononuclear subunit $[La(1,3\text{-}Hpdta)]_n$ of $[La(1,3\text{-}Hpdta)]_n{\cdot}nH_2O$ (**15**) in 30% thermal ellipsoids.

Figure 8. The infinite 3D structure of $[La(1,3\text{-}Hpdta)]_n{\cdot}nH_2O$ (**15**).

Fugure 9. Dimeric neutral unit $[Sm_2(Hpdta)_2(H_2O)_2]_n$ of $[Sm(1,3\text{-}Hpdta)(H_2O)]_n{\cdot}4nH_2O$ (**19**) in 30% thermal ellipsoids and infinite 2D layered structure.

Figure 10. Solution ^{13}C NMR spectra of **1** and $1,3\text{-}H_4pdta$.

Figure 11. TG curves of five types of lanthanide compounds.

Figure 12. Excitation and emission spectra of the europium coordination polymer **13** and **20**.

Scheme 1

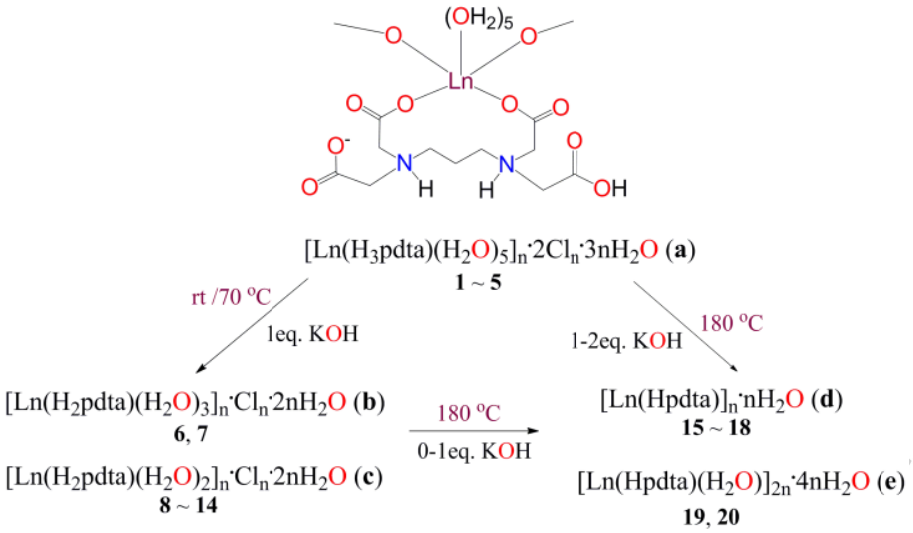

Figure 1

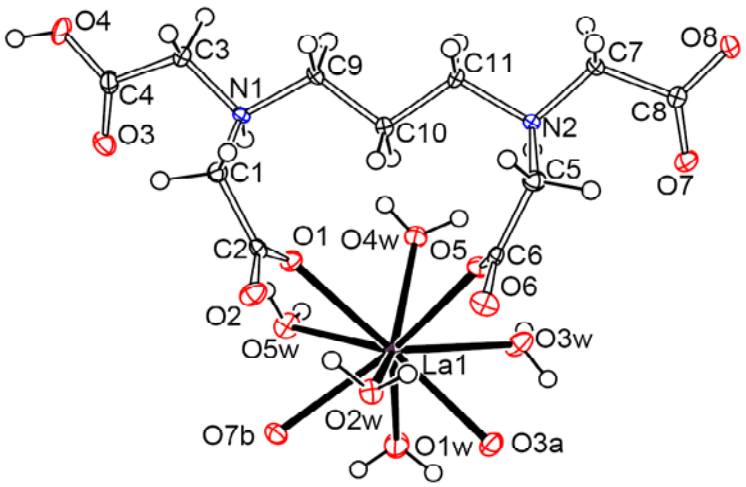

Figure 2

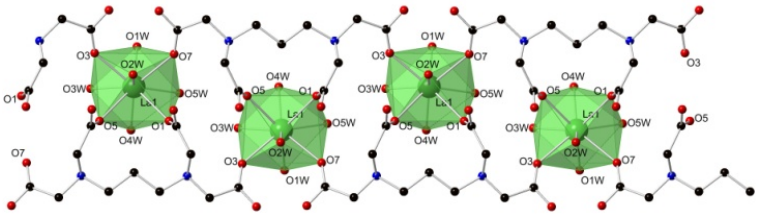

Figure 3

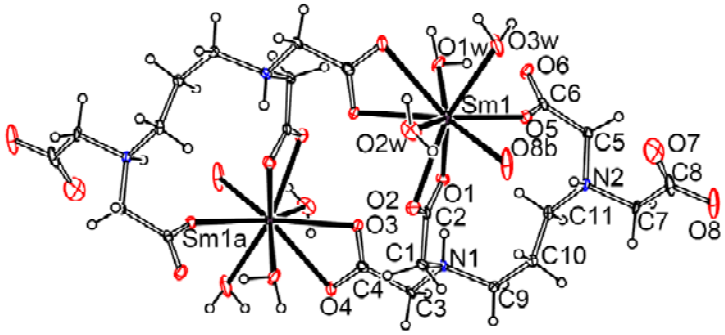

Figure 4

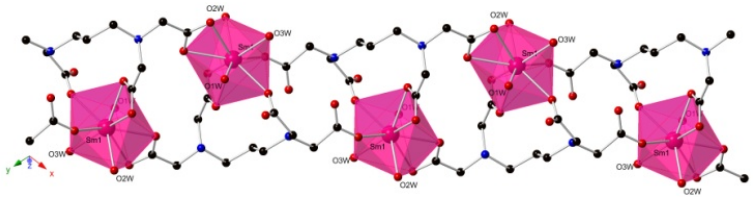

Figure 5

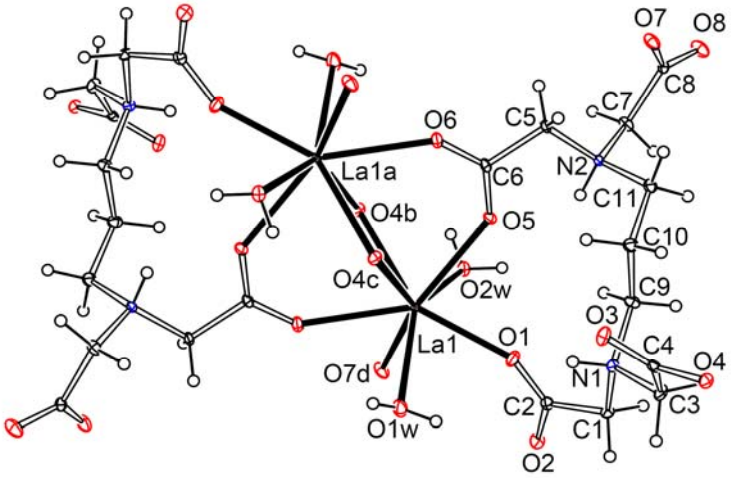

Figure 6

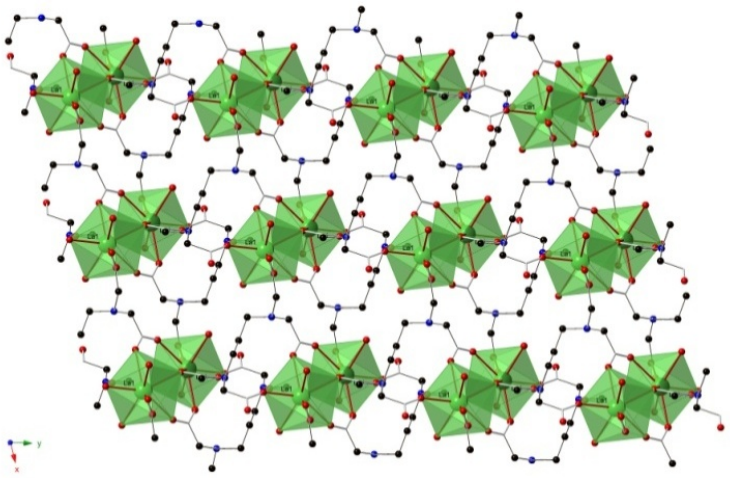

Figure 7

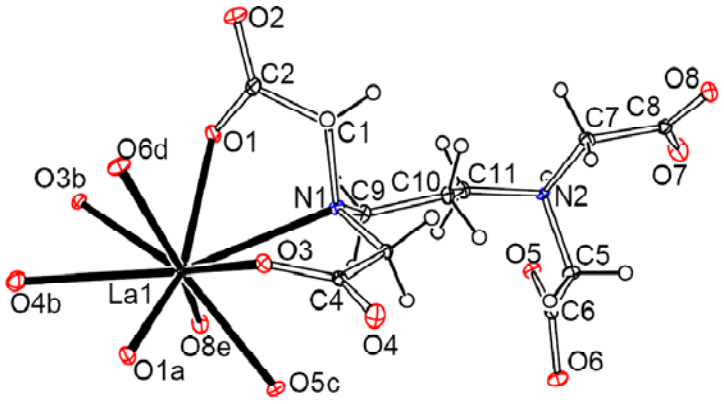

Figure 8

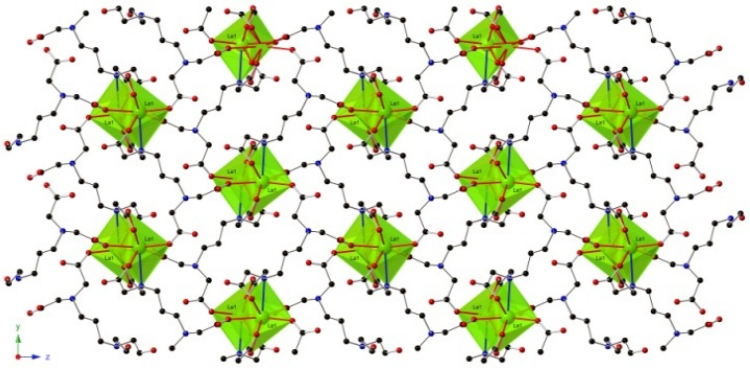

Figure 9

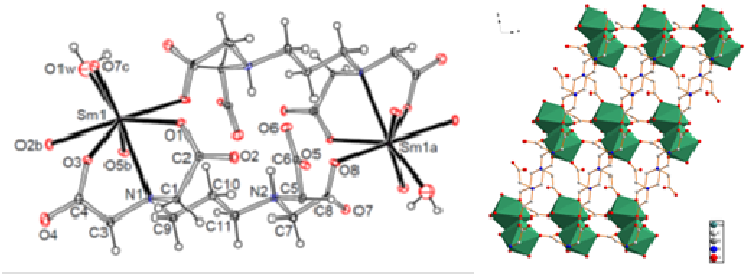

Figure 10

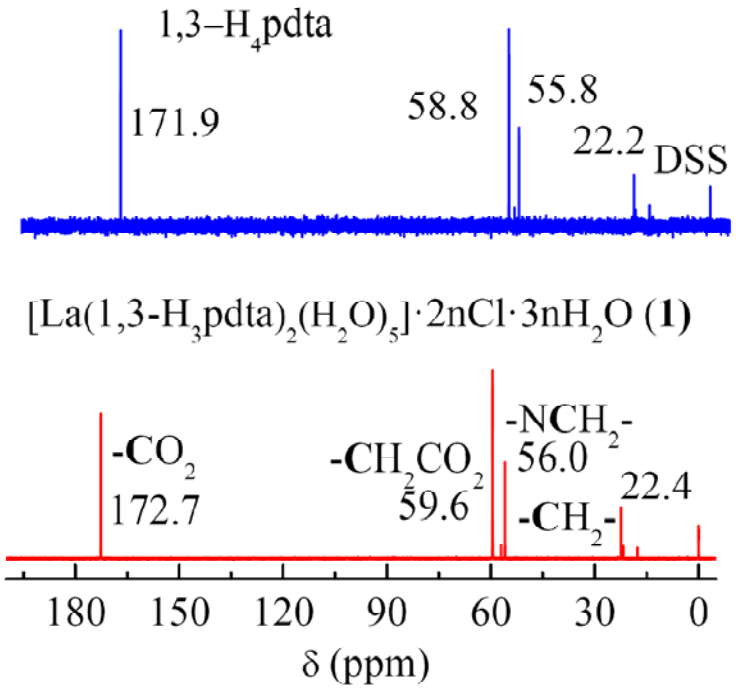

Figure 11

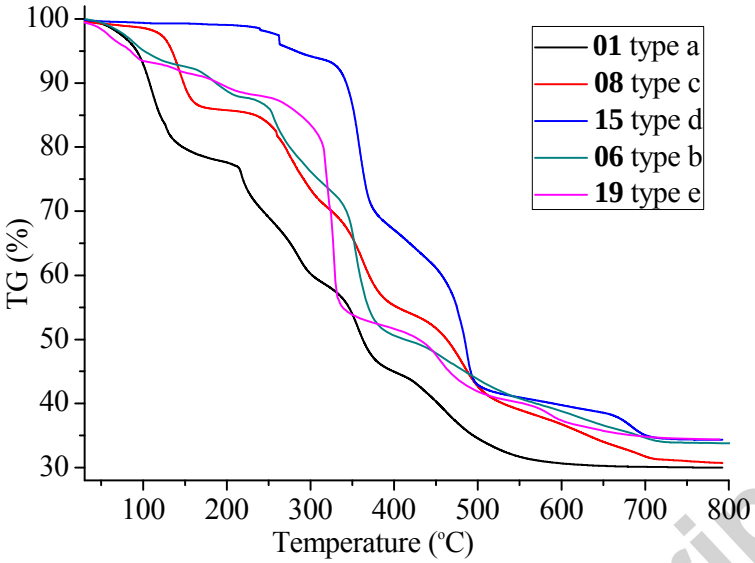

Figure 12

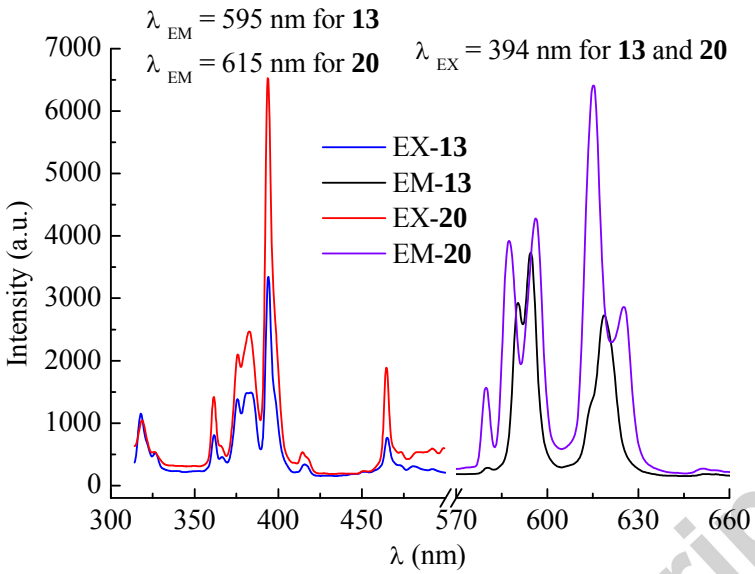

A series of water-soluble acidic 1,3-propanediaminetetraacetato lanthanides [Ln(1,3-H_3pdta)$(H_2O)_5$]n·2Cl_n·3nH_2O have been converted to their 2D and 3D lanthanides, which are active for the catalytic conversion of ester hydrolysis.

Highlights

novel acidic propanediaminetetraacetato lanthanides > water-soluble 1D coordination polymers > Acidic conditions are suitable for the isolations of lanthanide complexes in different structures > **1** and **5** show good catalytic activity to ester hydrolysis > europium coordination polymers **13** and **20** give visible fluorescence

Graphical Abstract (TOC Figure)

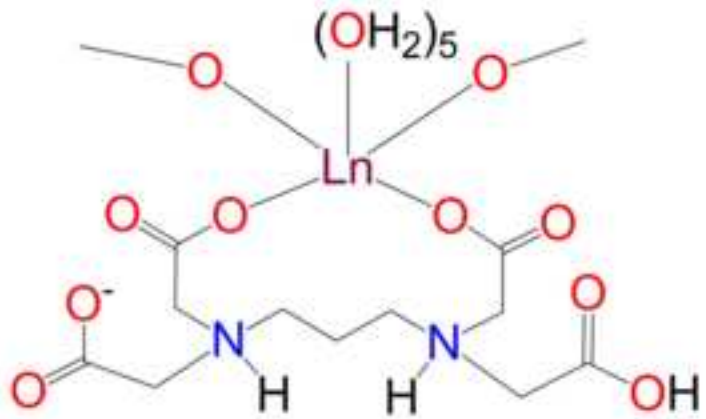

$[Ln(H_3pdta)(H_2O)_5]_n{\cdot}2Cl_n{\cdot}3nH_2O$ (**a**)

1 ~ 5

rt /70 °C

1eq. KOH

$[Ln(H_2pdta)(H_2O)_3]_n{\cdot}Cl_n{\cdot}2nH_2O$ (**b**)

6, 7

$[Ln(H_2pdta)(H_2O)_2]_n{\cdot}Cl_n{\cdot}2nH_2O$ (**c**)

8 ~ 14

180 °C

0-1eq. KOH

1-2eq. KOH

180 °C

$[Ln(Hpdta)]_n{\cdot}nH_2O$ (**d**)

15 ~ 18

$[Ln(Hpdta)(H_2O)]_{2n}{\cdot}4nH_2O$ (**e**)

19, 20